JOURNAL OF VIROLOGY, June 2009, p. 6211–6221 Vol. 83, No. 12
0022-538X/09/$08.00+0 doi:10.1128/JVI.00246-09

Polarization Restricts Hepatitis C Virus Entry into HepG2 Hepatoma Cells[▽]

Christopher J. Mee,[1] Helen J. Harris,[1] Michelle J. Farquhar,[1] Garrick Wilson,[1] Gary Reynolds,[2] Christopher Davis,[1] Sven C. D. van IJzendoorn,[3] Peter Balfe,[1]* and Jane A. McKeating[1]

Hepatitis C Research Group, Division of Immunity and Infection, University of Birmingham, Birmingham, United Kingdom[1]; Liver Laboratories, Institute for Biomedical Research, University of Birmingham and University Hospital Birmingham NHS Foundation Trust, Birmingham, United Kingdom[2]; and Department of Cell Biology/Membrane Cell Biology, University Medical Centre Groningen, University of Groningen, Groningen, The Netherlands[3]

Received 4 February 2009/Accepted 31 March 2009

The primary reservoir for hepatitis C virus (HCV) replication is believed to be hepatocytes, which are highly polarized with tight junctions (TJ) separating their basolateral and apical domains. HepG2 cells develop polarity over time, resulting in the formation and remodeling of bile canalicular (BC) structures. HepG2 cells expressing CD81 provide a model system to study the effects of hepatic polarity on HCV infection. We found an inverse association between HepG2-CD81 polarization and HCV pseudoparticle entry. As HepG2 cells polarize, discrete pools of claudin-1 (CLDN1) at the TJ and basal/lateral membranes develop, consistent with the pattern of receptor staining observed in liver tissue. The TJ and nonjunctional pools of CLDN1 show an altered association with CD81 and localization in response to the PKA antagonist Rp-8-Br-cyclic AMPs (cAMPs). Rp-8-Br-cAMPs reduced CLDN1 expression at the basal membrane and inhibited HCV infection, supporting a model where the nonjunctional pools of CLDN1 have a role in HCV entry. Treatment of HepG2 cells with proinflammatory cytokines, tumor necrosis factor alpha and gamma interferon, perturbed TJ integrity but had minimal effect(s) on cellular polarity and HCV infection, suggesting that TJ integrity does not limit HCV entry into polarized HepG2 cells. In contrast, activation of PKC with phorbol ester reduced TJ integrity, ablated HepG2 polarity, and stimulated HCV entry. Overall, these data show that complex hepatocyte-like polarity alters CLDN1 localization and limits HCV entry, suggesting that agents which disrupt hepatocyte polarity may promote HCV infection and transmission within the liver.

Hepatitis C virus (HCV) poses a global health problem, with over 170 million infected individuals worldwide. The principal reservoir for HCV replication is believed to be hepatocytes in the liver. Innate and adaptive cellular immune responses are thought to play a critical role in controlling HCV replication. However, in the majority of cases, the virus persists and the resulting hepatitis leads to progressive liver injury, frequently culminating in fibrosis and hepatocellular carcinoma. At the present time there is no vaccine and the only established treatment is alpha interferon (IFN-α) in combination with ribavirin, which is only partially effective. Hence, there is an urgent need for the development of more effective therapies.

The recent discovery that some strains of HCV can replicate in cell culture (HCVcc) and release infectious particles has allowed the complete viral life cycle to be studied (30, 52, 58). HCV initiates infection by attaching to molecules or receptors at the cell surface, and current evidence suggests that the tetraspanin CD81 (3, 10, 20, 26), scavenger receptor class B member I (SR-BI) (2, 22, 48), and the tight junction (TJ) proteins claudin-1 (CLDN1) and occludin (OCLN) (15, 37, 43, 55, 57) are required for HCV entry (reviewed in reference 50). However, the exact role(s) played by each of the receptors is unclear.

Many tissues in the body contain polarized cells, and hepatocytes are known to be highly polarized, with TJs regulating the paracellular transit of solutes. TJs comprise multiple transmembrane (CLDNs, OCLN, and the junctional adhesion molecule [JAM]), scaffolding, and signaling proteins (reviewed in reference 40). CLDNs belong to a large family of transmembrane proteins that oligomerize and form TJ strands that encircle the apical region of the cell. In addition, CLDNs can act as adhesion molecules, forming homodimeric and heterodimeric associations between adjacent cells (42), raising questions with respect to their accessibility to HCV particles and their role in the virus internalization process. To address the role of polarization in HCV entry, we previously utilized the well-characterized colorectal adenocarcinoma Caco-2 cell line and demonstrated that disrupting epithelial barrier formation increased HCV entry, suggesting that TJs impose a physical barrier and restrict viral access to receptors (36).

Most epithelial cells, including Caco-2, exhibit a simple polarity consisting of single apical and basal surfaces that oppose each other, with lateral surfaces participating in cell-cell associations. In vitro studies commonly use cell monolayers grown on semipermeable membranes, providing access to both the apical and basolateral domains. However, hepatocytes in the liver are polygonal and multipolar and do not possess the columnar morphology of simple epithelial cells, with at least two basal surfaces facing the circulation and a branched network of grooves between adjacent cells constituting the apical or bile canalicular (BC) surface. Thus, simple epithelial cell systems may fail to recapitulate the more complex hepatic

* Corresponding author. Mailing address: University of Birmingham, Division of Immunity and Infection, IBR, Vincent Drive, Birmingham B15 2TT, United Kingdom. Phone: (44) 121 414 8174. Fax: (44) 121 414 3599. E-mail: p.balfe@bham.ac.uk.

▽ Published ahead of print on 8 April 2009.

polarity that HCV will encounter in the liver. The majority of immortalized hepatocyte-derived cell lines and primary hepatocytes dedifferentiate in culture and fail to demonstrate a complex polarized phenotype. However, several studies have reported that the human HepG2 hepatoblastoma line develops hepatic polarity in culture, forming apical cysts that are equivalent to BC in the liver (reviewed in reference 13). Thus, we have utilized the HepG2 cell line to investigate the effect(s) of polarity on HCV infection.

Our studies demonstrate that HepG2 cells develop functionally active TJs and complex hepatic polarity that limit HCV entry. As HepG2 cells polarize, discrete pools of CLDN1 at the TJ and basal/lateral membranes develop, consistent with the pattern of receptor staining noted for liver tissue. The TJ and nonjunctional pools of CLDN1 show an altered association with CD81 and localization in response to the protein kinase A (PKA) antagonist (Rp-8-Br-cyclic AMPs [cAMPs]). The observation that Rp-8-Br-cAMPs reduce CLDN1 expression at the basal membrane and inhibit HCV infection supports a model where the nonjunctional pools of CLDN1 have a role in HCV entry. Treatment of HepG2 cells with proinflammatory cytokines, TNF-α and IFN-γ, perturbed TJ integrity but had minimal effect(s) on cellular polarity and HCV infection, suggesting that the integrity of TJs does not restrict HCV entry into polarized HepG2 cells. In contrast, activation of PKC with phorbol ester reduced TJ integrity, ablated HepG2 polarity, and stimulated HCV entry. Overall, these data show that complex polarity limits HCV entry, suggesting that agents which disrupt hepatocyte polarity may promote HCV infection and transmission within the liver.

MATERIALS AND METHODS

Cell lines and antibodies. HepG2, Huh-7, and Huh-7.5 cells were maintained in Dulbecco's modified Eagle's medium (DMEM) supplemented with 10% fetal bovine serum and 1% nonessential amino acids at 37°C and 5% CO_2. Primary human hepatocytes (PHH) were isolated and cultured as previously reported (41). HepG2 cells with aberrant E-cadherin distribution that lack functional adherens junctions (HepG2 AJ$^-$) were developed as previously reported (51) and cultured as described above in the presence of 1 mg/ml G-418 (Invitrogen, United Kingdom). Huh-7 and Huh-7.5 cells were kindly provided by Tianyi Wang (University of Pittsburgh, PA) and Charles Rice (Rockefeller University, New York, NY), respectively. HepG2 and HepG2 AJ$^-$ cells were seeded at 4×10^4 to 6×10^4 cells/cm^2, and Huh-7 and Huh-7.5 cells were seeded at 1.5×10^4 to 3×10^4 cells/cm^2 on plastic or glass coverslips, depending on the assay being performed. HepG2 cells expressing CD81, DsRED.CD81, and AcGFP.CLDN1 were generated by lentiviral transduction as previously described (24).

The following primary antibodies were used: anti-multidrug-resistant protein 2 (MRP2) (M2 III-6; Abcam Cambridge, United Kingdom), anti-NS5A 9E10 (C. Rice, Rockefeller University, NY), anti-CD81 (2s131), anti-SRBI (S. Shaw, Pfizer), anti-OCLN (Zymed, CA), anti-CLDN1 JAY.8 (Invitrogen, CA), anti-CLDN1 1C5-D9 (Novus, CO), and anti-ZO-1 (Zymed, CA). The following secondary-labeled antibodies were obtained from Invitrogen, CA: Alexa Fluor 488 goat anti-mouse immunoglobulin G (IgG), Alexa Fluor 488 goat anti-rabbit IgG, Alexa Fluor 633 goat anti-mouse IgG, and Alexa Fluor 633 goat anti-rabbit IgG.

Cell polarity determination. HepG2 cells and PHH were grown on 13-mm-diameter borosilicate glass coverslips (Fisher Scientific, United Kingdom) to the time point required and fixed in 3% paraformaldehyde at room temperature for 30 min. Cells were stained with anti-MRP2 in 0.1% Triton (Sigma Aldrich, United Kingdom), 0.5% bovine serum albumin (BSA) in phosphate-buffered saline (PBS), and Alexa Fluor 488-conjugated goat anti-mouse. Cell nuclei were visualized using 4′,6′-diamidino-2-phenylindole (DAPI; Invitrogen). The polarity index was determined by counting the number of MRP2-positive apical structures per 100 nuclei by using a Nikon Eclipse TE2000-S fluorescence microscope.

Determination of TJ "barrier" and "fence" functions. To determine the functionality of TJs and whether they restrict the paracellular diffusion of solutes from the BC lumen to the basolateral medium (barrier function), HepG2 cells were incubated with 5 μM 5-chloromethylfluorescein diacetate (CMFDA; Invitrogen) at 37°C for 10 min to allow internalization and translocation to the BC lumen by MRP2. After washing with PBS extensively, the capacity of BC lumens to retain CMFDA was analyzed using a fluorescence microscope.

To examine the fence function of TJs, HepG2 cells were cooled to 0°C with ice-cold PBS and incubated with 4 μM *N*-(*N*-[6-[(7-nitrobenz-2-oxa-1,3-diazol-4-yl)amino]caproyl])-sphingosylphosphorylcholine (C_6-NBD-SM) for 30 min to label the basolateral plasma membrane while preventing endocytosis. Cells were inspected under a fluorescence microscope to assess whether the fluorescent lipids had diffused from the basolateral surface to the BC surface membrane or if they had remained at the basolateral plasma membrane, indicating an intact TJ fence function.

HCVpp generation and infection. Pseudoviruses were generated by transfecting 293T cells (American Type Culture Collection, Manassas, VA) with two plasmids, one encoding a human immunodeficiency virus provirus expressing luciferase and the other encoding HCV strain H77 E1E2 region, the murine leukemia virus (MLV) envelope, or a no-envelope control as previously described (26). Supernatants were harvested at 48 h posttransfection, clarified, and filtered through a 0.45-μm membrane. Virus-containing medium was added to target cells plated as described above and incubated for 8 h, and unbound virus was removed and the medium replaced with DMEM containing 3% fetal bovine serum. At 72 h postinfection, the medium was removed and cells were lysed with cell lysis buffer (Promega, Madison, WI). Luciferase activity was assayed by the addition of the luciferase substrate, and measurements were taken for 10 s in a luminometer (Lumat LB 9507). Specific infectivity was calculated by subtracting the mean no-envelope control pseudoparticle signal from the HCV pseudoparticle (HCVpp) or MLVpp signals. Infectivity was presented relative to that of untreated control cells; i.e., the mean luciferase value (relative light units [RLU]) of the replicate untreated cells was defined as 100%.

HCVcc generation and infection. Stocks of J6/JFH virus were generated as previously described (30). Briefly, RNA was transcribed in vitro from full-length genomes using the MEGAscript T7 kit (Ambion) and electroporated into Huh-7.5 cells. Seventy-two and 96 h postelectroporation, supernatants were collected and stored immediately at −80°C. Virus containing medium was added to target cells plated as described above, and infected cells were detected by methanol fixation and staining for NS5A with anti-NS5A MAb 9E10 and Alexa 488-conjugated anti-mouse IgG. Infection was quantified by enumerating NS5A-positive foci, and infectivity was defined as the number of focus-forming units/milliliter. The infectious titer of early nonadapted J6/JFH for HepG2-CD81 cells was reduced 724-fold compared to the more permissive Huh-7.5 cell line.

Pharmacological treatments and compounds. Cells were plated as described above either on glass coverslips or cell culture plastic, depending on the assay being undertaken. Cells were serum starved for 4 h and treated with the following inhibitor and stimulator concentrations that were shown to be nontoxic (data not shown): 10 μM forskolin (FK) in the presence of 500 μM 3-isobutyl-1-methylxanthine (Sigma, United Kingdom), 10 ng/ml human oncostatin M (OSM; Cell Concepts, Germany); 1 mM dibutyryl cAMP (dbcAMP; Calbiochem, United Kingdom); 1 mM 8-(4-chlorophenylthio adenosine-3′, 5′-cyclic monophosphorothioate Rp-isomer (Rp-8-CPT-cAMPs; BioLog, Germany), and 8-bromoadenosine-3′, 5′-cyclic monophosphorothioate Rp-isomer (Rp-8-Br-cAMPs; BioLog, Germany). The control used in these experiments was dimethyl sulfoxide (DMSO; Sigma, United Kingdom) at a 1:1,000 dilution. For the Rho kinase inhibitor Y-27632 (Sigma, United Kingdom), cells were incubated with 2.5 μM Y-27632 for 24 h. For treatment with cytokines, cells were exposed to 10 ng/ml TNF-α (PeproTech, United Kingdom), 10 ng/ml IFN-γ (PeproTech, United Kingdom), 50 ng/ml of phorbol-12-myristate-13-acetate (PMA; Sigma, United Kingdom), or control PBS for 24 h before experimentation.

Immunohistochemistry. Representative 3-μm sections were cut from paraffin-embedded blocks of formalin-fixed tissue, placed onto charged slides, and incubated for 1 h at 60°C. Sections were dewaxed and rehydrated, and endogenous peroxidase was blocked with 0.3% hydrogen peroxide in distilled water. The tissue was subjected to an agitated low-temperature epitope retrieval technique as previously described (45). Sections were mounted onto a Shandon sequencer, blocked in 2% casein, and incubated with saturating concentrations of monoclonal antibodies (MAbs) specific for CD81 (2s131), CLDN1 (Zymed; Invitrogen), and OCLN (Zymed; Invitrogen) or control-irrelevant IgG diluted in Tris-buffered saline-0.1% Tween (TBS-Tween) for 1 h. After a TBS-Tween wash, sections were incubated with an ImPress Universal anti-mouse IgG/anti-rabbit IgG peroxidase kit (Vector Labs). After being washed further with TBS-Tween, bound antibodies were visualized by using ImPact DAB diluent and a chromogen kit

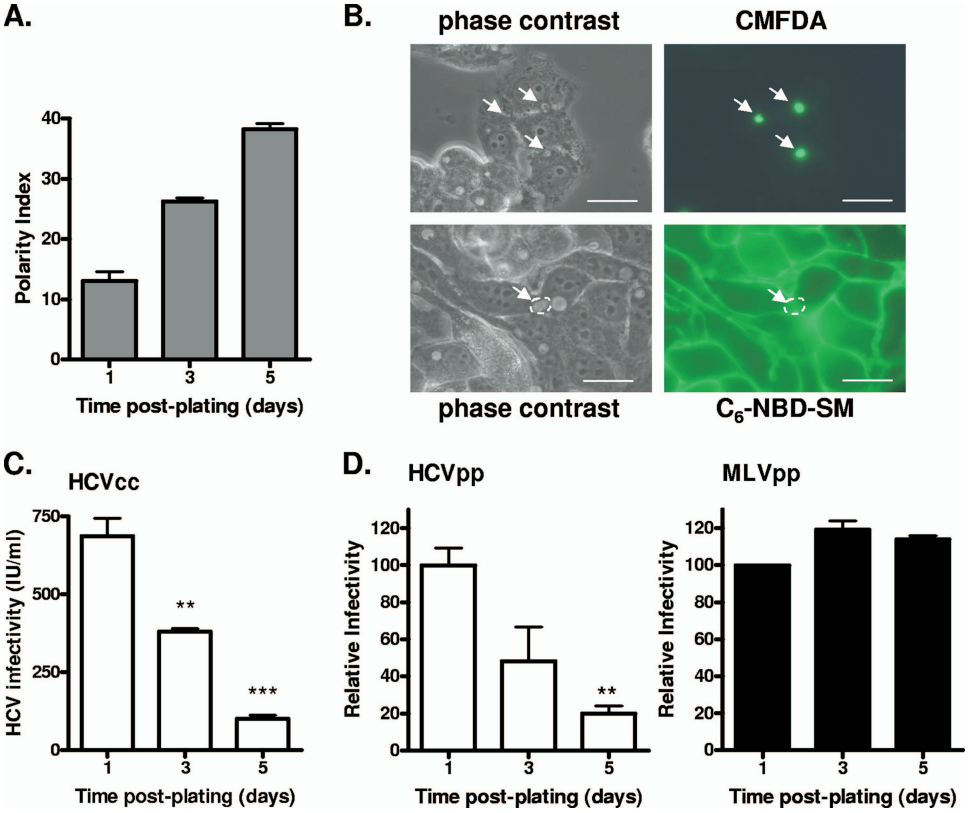

FIG. 1. Effect of HepG2 polarity on HCV entry. (A) HepG2 cells were grown for 1, 3, or 5 days, fixed in 3% paraformaldehyde, and stained for the BC-expressed marker MRP2. The polarity index was assessed by quantifying the number of MRP2-positive BC per 100 cell nuclei for five fields of view on three replicate coverslips. (B) The BC in polarized HepG2 cells were assessed for both "barrier" and "fence" functions. Cells were incubated with either C_6-NBD-SM, to measure fence function, or CMFDA, which measures barrier function. Restriction of C_6-NBD-SM to the basal plasma membrane and restriction of CMFDA to the BC indicate that polarized HepG2 cells have functional TJs. (C) HCVcc J6/JFH was used to infect HepG2-CD81 cells at 1, 3, or 5 days postplating. Infected cells were visualized after 72 h (NS5A staining), and infectivity (focus forming units/milliliter) was calculated. **, $P < 0.001$; ***, $P < 0.0001$ (*t* test). (D) HCVpp (white bars) and MLVpp (black bars) infection of HepG2-CD81 cells at 1, 3, or 5 days postplating. Infectivity is expressed relative to HepG2 cells infected immediately after plating ± SD. **, $P < 0.001$ (*t* test). HCVpp infectivity values for HepG2-CD81 and HepG2 cells after 1 day of plating were 20,753 ± 1,060 RLU and 360 ± 12 RLU; MLVpp infectivity values for HepG2-CD81 and HepG2 cells were 140,187 ± 483 RLU and 143,471 ± 517 RLU.

(Vector Labs) and counterstained with hematoxylin. Images were obtained using a Nikon Eclipse E400 microscope. Acetone-fixed frozen sections of normal tissue were stained in a comparable manner to confirm the pattern of CD81, CLDN1, and OCLN expression had not been altered during paraffin wax processing and formalin fixation.

Confocal microscopy. HepG2 cells were grown on 13-mm-diameter borosilicate glass coverslips (Fisher Scientific, United Kingdom) and fixed in 3% paraformaldehyde (for anti-CD81 2s131) or ice-cold methanol (for all other antibodies). Cells were permeabilized for 30 min in 0.05% saponin and 0.5% BSA in PBS and incubated with primary antibodies for 1 h at room temperature in PBS-saponin-BSA. Cells were washed three times in PBS-saponin-BSA before addition of the appropriate Alexa 488-conjugated anti-species IgG diluted to 1:1,000 in PBS-saponin-BSA for 1 h at room temperature. Cells were washed three times in PBS-saponin-BSA before being counterstained with DAPI (Invitrogen) in PBS for 5 min. Coverslips were mounted on glass slides (ProLong Gold antifade; Invitrogen) and viewed by laser-scanning confocal microscopy (LSCM) on a Zeiss META head confocal microscope with a ×63 water-immersion objective.

Quantification of AcGFP.CLDN1 and DsRED.CD81 expression and FRET association. HepG2 cells transduced to express AcGFP.CLDN1 and DsRED.CD81 were grown on 13-mm glass coverslips and fixed in ice-cold methanol, and the TJ location was identified by costaining for OCLN or ZO-1. The cells were imaged by LSCM, with the microscope settings optimized for each fluorescent protein to obtain the highest signal-to-noise ratio. The intensity of AcGFP.CLDN1 and DsRED.CD81 expression (arbitrary fluorescence units/pixel) at the plasma membrane of nonpolarized cells and the basal and lateral membranes and TJs of polarized cells provides 500 to 1,000 measurements per cell. The data from 10 cells were normalized, and the localized expression was calculated. For fluorescent resonance energy transfer (FRET) analysis, the gradual acceptor photobleaching method of FRET was used, which entailed photobleaching the DsRED fluorophore gradually over time while monitoring AcGFP fluorescent intensity, as previously described (24). After background and cross-talk correction, any increase in AcGFP intensity following DsRED photobleaching is due to FRET between the proteins, implying a distance of less than 10 nm. Each pixel has an AcGFP and DsRED fluorescent intensity that may increase or decrease following acceptor photobleaching. The percent FRET is defined as the number of pixels that display FRET over the total number of pixels analyzed.

Statistical analysis. Results are expressed the mean ± 1 standard deviation of the mean (SD), except where stated to the contrary. Statistical analyses were performed using Student's *t* test in Prism 4.0 (GraphPad, San Diego, CA), with a P value of <0.05 being considered statistically significant.

RESULTS

Effect of polarization on HCV entry. We previously reported that HepG2 cells transduced to express CD81 support HCVpp infection, and we utilized these cells to study the effect(s) of polarity on HCV entry. HepG2-CD81 cells formed an increasing number of BC over time, with approximately 38 BC detected per 100 cells at 5 days postplating (Fig. 1A). Since at least two cells participate in the formation of one BC, this corresponds to at

least 76% of the cells developing an apical membrane. CD81 expression did not alter the ability of HepG2 cells to polarize (data not shown). To test the functionality of TJs, we investigated the retention of BC-localized CMFDA and basolateral membrane-associated C_6-NBD-SM lipids. Eighty percent of BC retained CMFDA, and a similar percentage of cells maintained basolateral localized C_6-NBD-SM (Fig. 1B), demonstrating that HepG2-CD81 cells develop "barrier" and "fence" TJ activities.

To study the effect(s) of polarization on HCVcc infection, we monitored the ability of J6/JFH to infect HepG2-CD81 cells at 1, 3, and 5 days postplating. As the percentage of polarized cells in the culture increased, the frequency of cells supporting HCVcc infection declined (Fig. 1C). Due to the low permissivity of HepG2 cells in supporting HCV RNA replication (12), experiments were performed at a low multiplicity of infection (MOI; 0.01 to 0.05). To ascertain if the reduced frequency of NS5A-expressing cells in the polarized cultures was due to differences in the HCV glycoprotein-dependent entry, we studied the ability of HCVpp and control MLVpp to infect HepG2-CD81 cells seeded at various times. Polarization limits HCVpp infection, whereas MLVpp infection was unaffected, demonstrating that the HCV glycoprotein-dependent entry is reduced in polarized HepG2 cells (Fig. 1D).

To ascertain whether PHH polarize and form BC structures, the cells were stained for the apical markers MRP2 and CD26. A low frequency of BC was observed in two independent donor preparations, suggesting that less than 5% of hepatocytes were polarized. These data are consistent with reports in the literature that cultured hepatocytes show limited evidence of BC morphogenesis (reviewed in reference 13). Both PHH cultures supported J6/JFH replication as judged by reverse transcription-PCR determination of HCV RNA relative to a cellular housekeeping gene (glyceraldehyde-3-phosphate dehydrogenase [GAPDH]) (36). At 48 h postinfection, differences between HCV and GAPDH amplification threshold values of 9.3 (PHH donor 1), 10.23 (PHH donor 2), and 8.74 (Huh-7.5 cells) were obtained, demonstrating that PHH support HCV replication at levels comparable to those of Huh-7.5 cells.

Several reports have highlighted the importance of PKA in regulating cell polarity and the trafficking of proteins and lipids to polarized cell surfaces. The decreased susceptibility of HepG2-CD81 cells to virus over time suggests that HCV is less able to enter polarized cells; however, other parameters may have been modulated during their time in culture. To independently study the effect of polarization on viral entry, we examined the effect of PKA agonists and the interleukin-6 family cytokine OSM on HCVpp entry. HepG2-CD81 cells (3 days postplating) were treated for 1 h with FK, which activates adenylyl cyclase and increases intracellular cAMP, exogenous dbcAMP, or OSM and were assessed for BC formation and susceptibility to HCVpp infection. All of the treatments promoted HepG2-CD81 polarization and induced a significant decrease in HCVpp entry with minimal effect(s) on MLVpp infection (Fig. 2A to B). In contrast, the various agents had no detectable effect on HCVpp infection of Huh-7 or Huh-7.5 cells (data not shown). To confirm that the effect(s) of dbcAMP on HCVpp entry is not due to the toxic effects of free butyrate, cells were treated with an increasing concentration(s) of dbcAMP in the presence or absence of the selective PKA holoenzyme antagonist, Rp-8-CPT-cAMPs. Treatment with

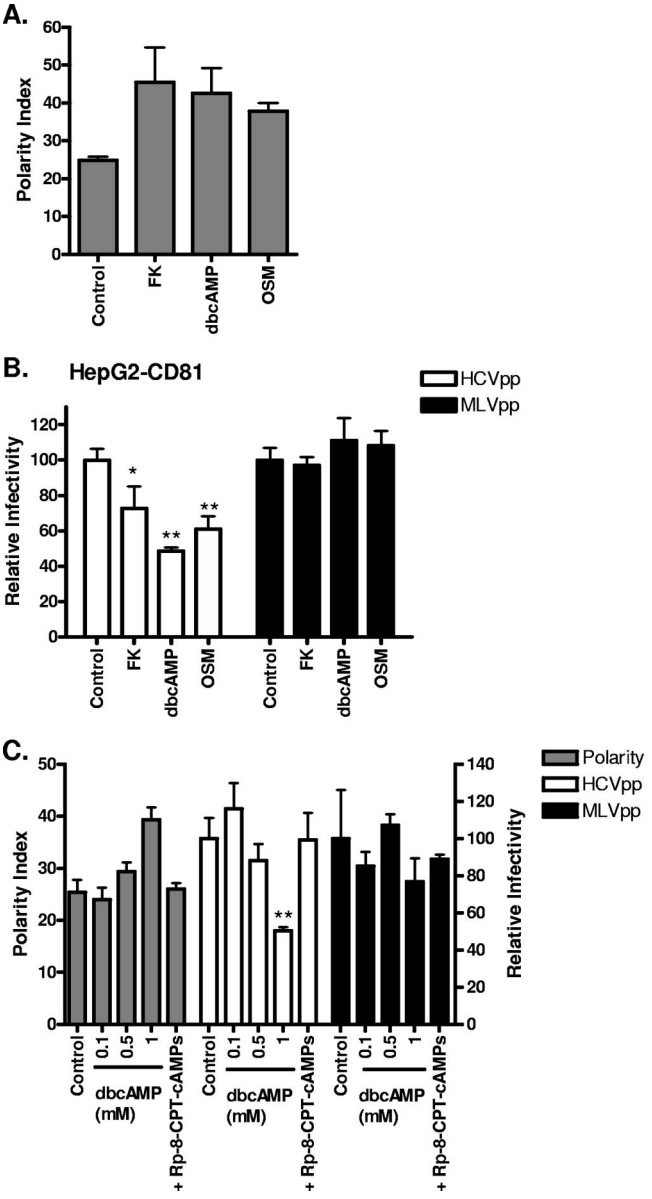

FIG. 2. PKA stimulation of HepG2 polarity reduces HCV entry. (A) Polarized HepG2-CD81 cells grown for 3 days were treated with serum-free DMEM for 4 h before being exposed to FK (10 μM), dbcAMP (1 mM), OSM (10 ng/ml), or control (DMSO; 1:1,000) for 1 h. Cells were fixed, and their polarity indexes were measured. (B) HCVpp (white bars) or MLVpp (black bars) infection of polarized HepG2-CD81 cells (3-day culture) after treatment with FK (10 μM), OSM (10 ng/ml), dbcAMP (1 mM), or control (DMSO; 1:1,000) for 1 h. Infectivity is expressed relative to control-treated cells ± SD. *, $P < 0.01$; **, $P < 0.001$ (*t* test). (C) Polarity (gray bars) and HCVpp (white bars) or MLVpp (black bars) infection of HepG2-CD81 cells following treatment with control (DMSO; 1:1,000), dbcAMP (0.1, 0.5, and 1 mM), or 1 mM dbcAMP and 1 mM Rp-8-CPT-cAMPs. Cells were treated with compounds for 1 h, following a 4-h incubation in serum-free DMEM. The polarity index was measured as previously described (left *y* axis). HCVpp and MLVpp infection was assessed 72 h after treatment, and data are shown as relative infectivity (right *y* axis) calculated as a percentage of control cells ± SD. **, $P < 0.001$ (*t* test). HCVpp infectivity values for HepG2-CD81 and HepG2 cells were 23,350 ± 1,583 RLU and 447 ± 14 RLU; MLVpp infectivity values for HepG2-CD81 and HepG2 cells were 165,200 ± 158 RLU and 115,300 ± 177 RLU.

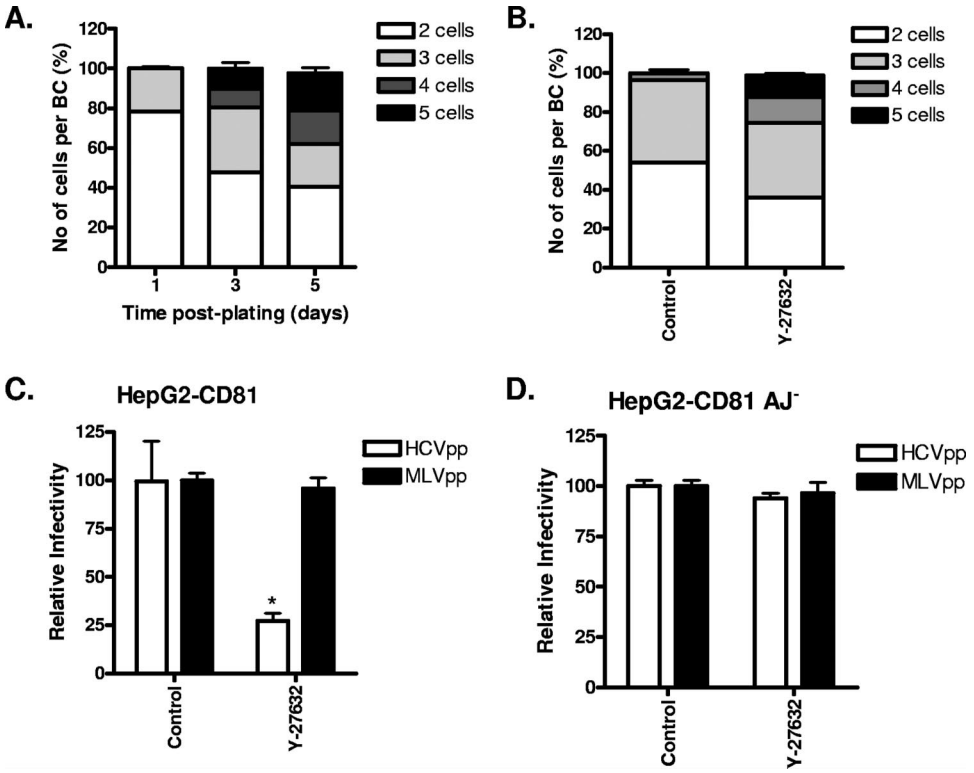

FIG. 3. Effect of complex HepG2 polarity on HCV entry. (A) Cells grown for 1, 3, or 5 days were stained to visualize BC, and the number of cells sharing a BC was enumerated. (B) HepG2-CD81 cells (1 day postplating) were treated with control (DMSO; 1:1,000) or Rho kinase inhibitor Y-27632 (2.5 μM) for 24 h. Cells were fixed, and the number of cells sharing a BC was counted. To investigate the effect of complex polarity on HCV entry, HepG2-CD81 (C) and HepG2-CD81 AJ$^-$ (D) cells (1 day postplating) were treated with the control or Y-27632 before being infected with HCVpp (white bars) or MLVpp (black bars) for 8 h. Data are shown as relative infectivity calculated as a percentage of control cells ± SD, where the mean infection value of the control cells is defined as 100%. *, $P < 0.01$ (*t* test). HCVpp infectivity values for HepG2-CD81 and HepG2 cells were 35,410 ± 3,219 RLU and 104 ± 4 RLU; MLVpp infectivity values for HepG2-CD81 and HepG2 cells were 335,343 ± 5,888 RLU and 354,100 ± 6,474 RLU.

dbcAMP induced a dose-dependent increase in polarity and a reduction in HCVpp entry that was ablated in the presence of the PKA antagonist (Fig. 2C). In summary, these data show that polarized HepG2 cells are less able to support HCV entry.

The mature hepatic phenotype observed in the adult liver develops during embryogenesis from nonpolarized hepatoblasts into clusters of cells that initially form isolated intercellular BC cavities and later form a branched BC network spanning multiple cells (19, 25, 34). The molecular mechanisms directing the conversion from simple to complex polarity and the BC organization of the adult liver are poorly defined. HepG2 cells develop complex polarity over time, with multiple cells sharing a common BC structure (Fig. 3A), providing an in vitro system to study HCV entry into polarized cells that may be more representative of the adult liver. Culturing cells on a predeposited extracellular matrix or inhibition of Rho kinase promotes the development of complex polarity (25). HepG2-CD81 cells were treated with the Rho kinase inhibitor (Y-27632), and the number of cells sharing a BC and their permissivity to HCVpp infection was assessed. Inhibition of Rho kinase led to a greater number of cells sharing a BC and a decline in the number of BC involving only two or three cells (Fig. 3B). The increased frequency of complex polarized cells in the population was associated with a significant reduction in HCVpp entry, with no detectable effect on MLVpp entry (Fig. 3C). In contrast, HCVpp or MLVpp infection of Huh-7 or Huh-7.5 cells was not modulated by prior treatment with Y-27632 (data not shown). HepG2 cells with aberrant E-cadherin distribution that lack functional adherens junctions (HepG2 AJ$^-$) fail to develop complex polarity in vitro (51). Y-27632 treatment of HepG2-CD81 AJ$^-$ cells had no effect on the number of cells sharing a BC or HCVpp and MLVpp infection (Fig. 3C). In summary, these data demonstrate that complex polarity restricts HCV entry into HepG2 cells.

Effect(s) of polarization on HCV receptor localization. Since polarization reduces the ability of HepG2 to support HCV entry, we were interested to study the effects of polarization on viral receptor localization. HCV receptor expression was assessed in nonpolarized and polarized HepG2-CD81 cells by LSCM. The TJ-associated proteins OCLN and ZO-1 were visible in polarized cells as a discrete band surrounding the BC structure, depending on the cellular orientation (Fig. 4A and data not shown). In contrast, CD81 and SR-BI demonstrated plasma membrane staining in nonpolarized HepG2-CD81 cells, with both coreceptors at apical/BC and basal and lateral membranes upon polarization (Fig. 4A). In nonpolarized cells, CLDN1 is expressed at the plasma membrane, and upon polarization the protein relocalizes to the TJ, with the staining

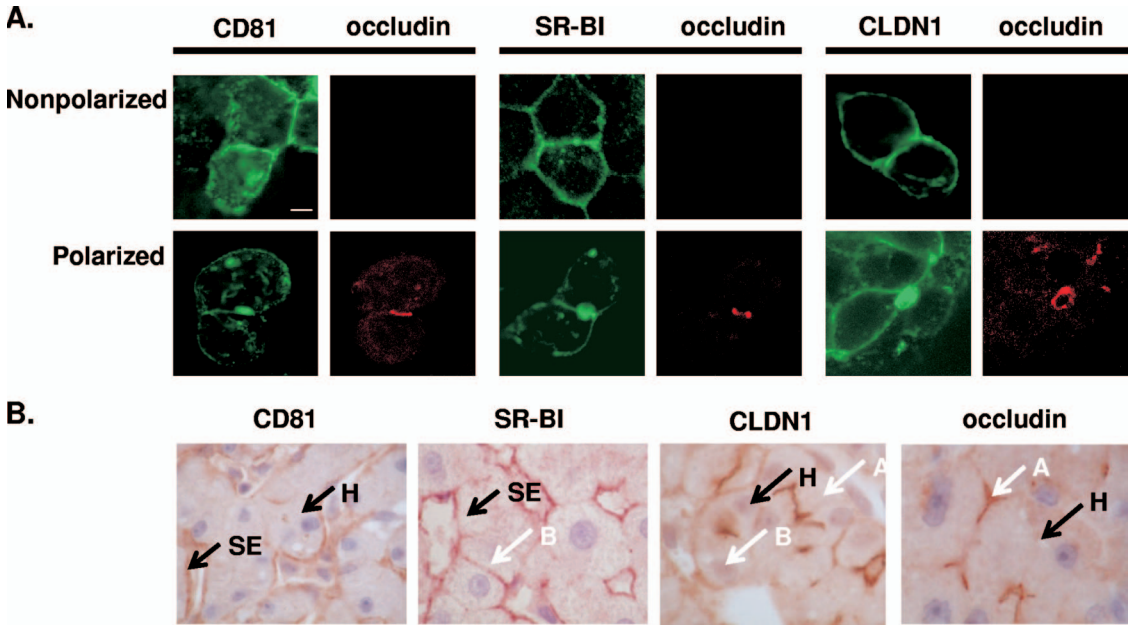

FIG. 4. Localization of viral receptors in HepG2 cells and liver tissue. (A) HepG2-CD81 cells were seeded onto glass coverslips at a density resulting in polarized and nonpolarized cells in the population. Cells were dual-stained with antibodies specific for CD81, SR-BI, CLDN1, and OCLN and visualized by confocal microscopy. Bar, 10 μm. (B) Liver sections (3 μm) were cut from paraffin blocks of formalin-fixed tissue and stained with mouse MAbs to CD81, SR-BI, CLDN1, and OCLN. Tissue morphology is shown by arrows, along with sinusoidal endothelium (SE), hepatocytes (H), and cell surfaces (white arrows) on apical canaliculi (A) and basolateral membranes (B).

intensity at the basal and lateral membranes decreasing (Fig. 4A). To ascertain whether our in vitro observations reflect receptor localization in vivo, we stained nondiseased liver tissue for CD81, SR-BI, CLDN1, and OCLN. Hepatocyte membranes stained uniformly for CD81 and SR-BI, and CLDN1 showed a dominant staining pattern at the BC and a lower staining intensity at basolateral membranes, whereas OCLN was detected only at the BC structures (Fig. 4B). Comparable staining patterns were observed with formalin-fixed and frozen liver tissue. In summary, these experiments show concordant CD81, SR-BI, CLDN1, and OCLN localization in polarized HepG2 cells and liver tissue.

We previously reported that FRET occurred between fluorescent-tagged versions of plasma membrane-expressed CLDN1 and CD81 in 293T and Huh-7.5 hepatoma cells, consistent with the formation of receptor complexes (24). To quantify the effect(s) of polarization on CLDN1 and CD81 localization and FRET association, HepG2 cells were transduced to express AcGFP.CLDN1 and DsRED.CD81. The pattern of AcGFP.CLDN1 staining in polarized HepG2 cells was comparable to that observed for endogenous CLDN1 (Fig. 5A). Transduced HepG2 cells were costained for OCLN to identify TJ structures, and the fluorescent intensity of CLDN1 and CD81 at the basal and lateral membranes and the TJs estimated. The level(s) of CLDN1 expressed at the basal and lateral membranes of polarized cells was comparable to that observed in nonpolarized cells (Fig. 5B). However, in the polarized cells, CLDN1 is more highly expressed at the TJs, whereas CD81 is more uniformly expressed in polarized and nonpolarized cells, with no elevated expression at the TJs (Fig. 5B). The percentage of FRET between basal membrane-expressed pools of AcGFP-CLDN1 and DsRed-CD81 in polarized HepG2 cells and plasma membrane-expressed proteins in nonpolarized cells was comparable (37.5% ± 4.7% and 41% ± 11.5%, respectively). In contrast, there was no detectable FRET between CLDN1 and CD81 at the TJs, suggesting that the conformation, density, or stoichiometry of either protein at this location is not compatible with coreceptor association. On the assumption that CLDN1-CD81 complexes are important for HCV entry (24, 55), these data lend further support for a role of nonjunctional pools of CLDN1 in HCV entry.

We previously reported that inhibiting PKA in Huh-7.5 cells induced a reorganization of CLDN1 from the plasma membrane to intracellular sites and inhibited HCV entry (16). To ascertain whether TJ and nonjunctional pools of CLDN1 in HepG2 cells are equally sensitive to the effect(s) of the PKA antagonist, Rp-8-Br-cAMPs, HepG2 cells stably expressing AcGFP.CLDN1 and DsRED.CD81 were treated for 1 h and the receptor localization was quantified. Inhibiting PKA had no detectable effect(s) on CD81 localization (data not shown), whereas Rp-8-Br-cAMPs modulated CLDN1 localization, leading to a loss in basal membrane expression and an increase in lateral- and TJ-associated forms (Fig. 6A to B). The treatment led to a fivefold reduction in CLDN1-CD81 FRET at the basal membrane (control, 39% ± 5.7%; Rp-8-Br-cAMPs, 8% ± 7.9%) and a significant decline in HCVpp entry (Fig. 6C) but no detectable effect on polarity (Fig. 6D). Since there was no detectable effect(s) of Rp-8-Br-cAMPs on CLDN1-CD81 FRET at the lateral or TJ domain, we tentatively conclude that the levels of CLDN1 expression at the basal membrane may limit HCV entry.

Cytokine modulation of HepG2 TJ integrity and HCV entry. To investigate a role for TJs in restricting entry of HCV into polarized HepG2 cells, we assessed the effect(s) of TNF-α and

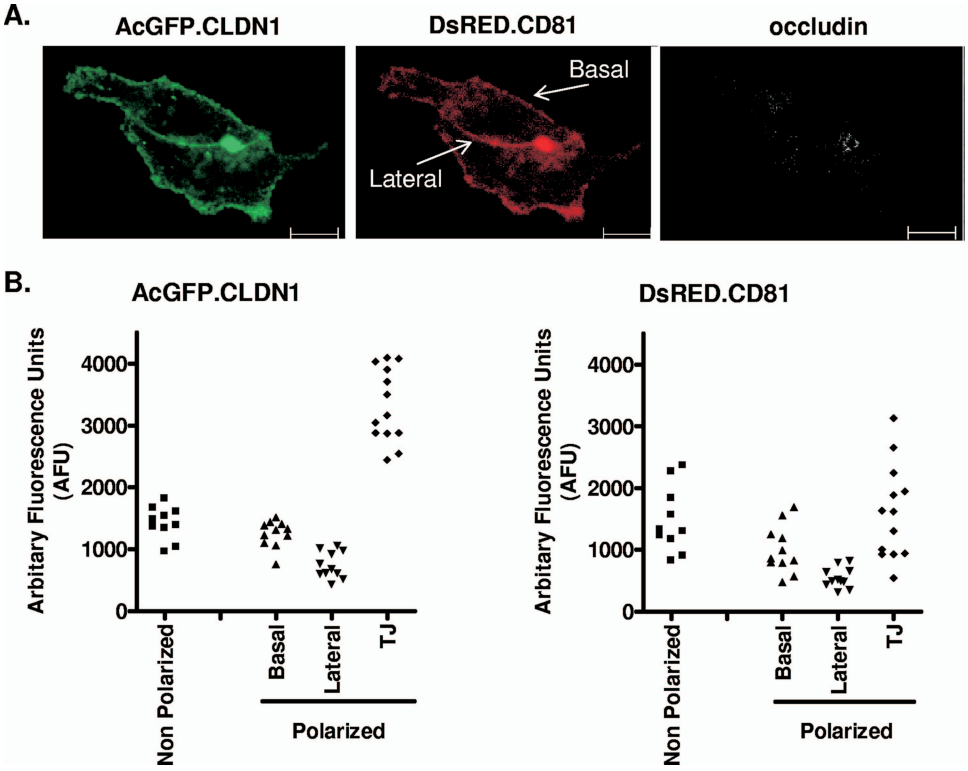

FIG. 5. Effect(s) of HepG2 polarization on CD81 and CLDN1 localization. (A) HepG2 cells transduced to express AcGFP.CLDN1 and DsRED.CD81 were seeded onto glass coverslips. The cells were fixed 1 day postplating, stained for TJs with an antibody to OCLN, and visualized by confocal microscopy. Bars, 20 μm. (B) Quantification of plasma membrane-expressed pools of AcGFP.CLDN1 and DsRED.CD81. Shown are scatter plots of AcGFP.CLDN1 and DsRED.CD81 fluorescent intensity/pixel/cell at plasma membrane locations in polarized and nonpolarized cells. Intensity is presented as arbitrary fluorescence units (AFU).

IFN-γ on HepG2-CD81 TJ integrity, polarity, and HCV entry. PKC activation is reported to mediate the disassembly of TJs in a variety of experimental systems (reviewed in reference 23), and we therefore treated cells with the PKC stimulator PMA. Both TNF-α and IFN-γ treatments reduced TJ integrity by approximately 50% (Fig. 7A) with no significant effect on polarity (Fig. 7B) or HCVpp entry (Fig. 7C). Neither treatment had a discernible effect on CLDN1, ZO-1, or OCLN localization (data not shown). In contrast, PMA abrogated TJ integrity and significantly reduced HepG2 polarity (Fig. 7A to B), with reduced expression of CLDN1, ZO-1, and OCLN at the TJs (data nor shown). PMA treatment of HepG2-CD81 enhanced HCVpp and HCVcc infection, with minimal effect on MLVpp entry (Fig. 7C and data not shown). Activation of PKC is likely to have pleiotropic effects on the cell, and it is interesting to note that PMA had no effect on HCVpp or MLVpp infection of Huh-7 or Huh-7.5 cells (Fig. 7D). We conclude that TJ integrity per se does not restrict HCV entry into polarized HepG2 cells and that cytokine-induced changes in TJs had a modest effect on HCV entry.

DISCUSSION

Polarity is characterized by a specific organization of plasma membrane proteins and defines the shape and architecture of a cell. Hepatocyte polarity requires the coordinated establishment and maintenance of TJs and apical membrane domains (6, 27, 56). We demonstrate that HepG2 polarization limits HCV entry (Fig. 1) and that treating cells with PKA agonist(s), OSM, and Rho kinase inhibitor Y-27632, which stimulate polarization via distinct modes of action (25), specifically reduce HCVpp infection (Fig. 2 and 3). HepG2 develops BC-like spaces that form elongated canalicular lumens spanning several cells (Fig. 3A to B) (25), and the resistance of HepG2-CD81 cells to HCVpp infection following Rho kinase inhibition suggests that membrane remodeling associated with canalicular development restricts viral entry (Fig. 3C). In contrast, canalicular structures were infrequently detected in cultured PHH (<5%), consistent with their rapid dedifferentiation in culture (reviewed in reference 53). We and others have reported that PHH support low-level HCVcc replication; however, it has been difficult to quantify the frequency of infected cells within the population and to study the role of polarity in HCV entry (reviewed in reference 17).

To ascertain whether the reduced permissivity of polarized HepG2 cells to HCV infection was due to a reorganization of the viral receptors, we imaged endogenous and fluorescent-tagged versions of CD81 and CLDN1. Both receptors localized to areas of cell-cell contact in nonpolarized cells, and the majority of CLDN1 redistributed to TJs upon polarization (Fig. 4 and 5). In contrast, ZO-1 and OCLN appeared to localize exclusively to TJs surrounding the BC (Fig. 4 and 5). CD81, SR-BI, CLDN1, and OCLN localization in polarized HepG2 cells was comparable to that observed in healthy liver

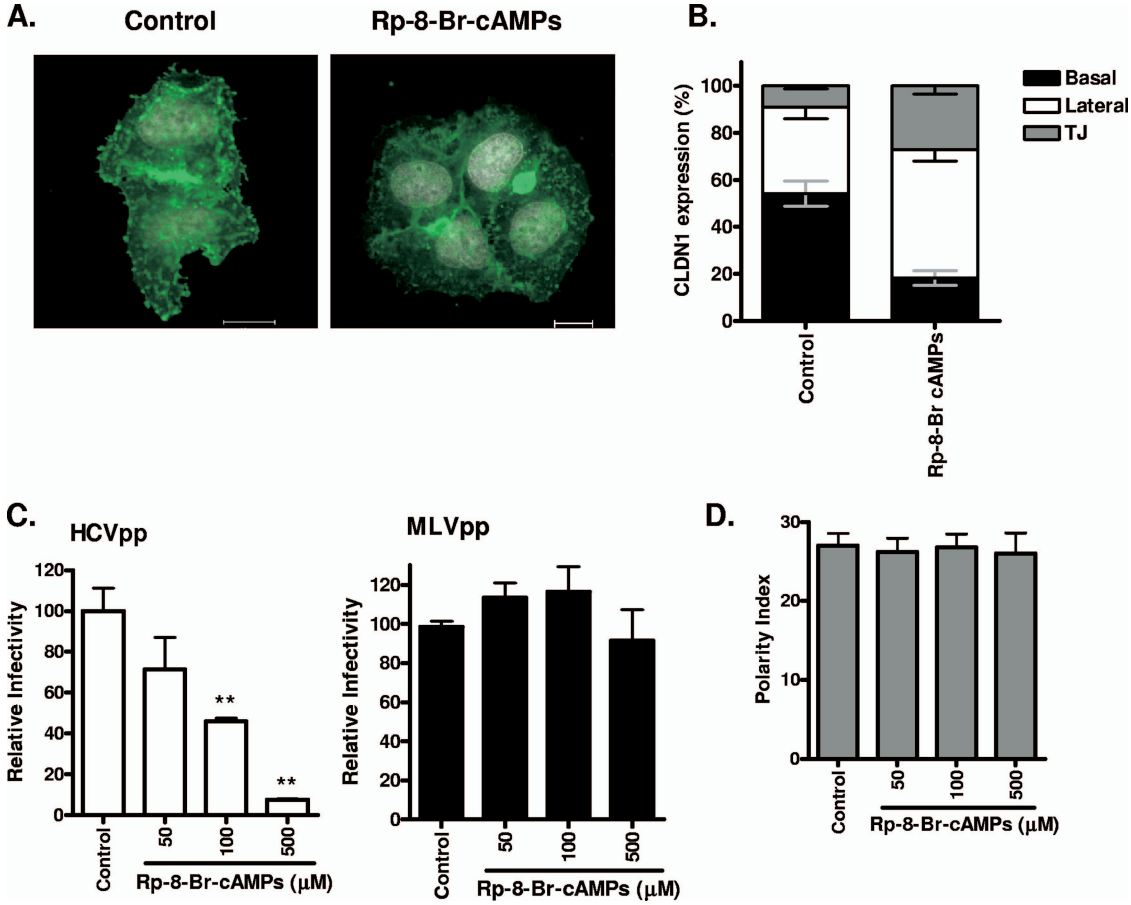

FIG. 6. Inhibition of PKA modulates basolateral pools of CLDN1 and HCV entry. (A) HepG2 cells transduced to express AcGFP.CLDN1 and DsRED.CD81 were seeded onto glass coverslips, and after 4 h in serum-free DMEM, they were treated with DMSO (control; 1:1,000) or Rp-8-Br-cAMPs (500 mM) for 1 h. Cells were visualized using confocal microscopy, and the CLDN1 localization was assessed. Bars, 20 μm. (B) Reorganization of AcGFP.CLDN1 after a 1-h treatment with control or Rp-8-Br-cAMPs (500 mM). The percentages of CLDN1 at the basal (black), lateral (white), and TJ (gray) locations were measured. (C) HCVpp (white bars) and MLVpp (black bars) infection of HepG2-CD81 cells (3 days postplating), following treatment with the control (1:1,000) or Rp-8-Br-cAMPs (50, 100, or 500 mM) for 1 h. Relative infectivity was calculated as a percentage of control cells ± SD. **, $P < 0.001$ (*t* test). HCVpp infectivity values for HepG2-CD81 and HepG2 cells were 14,710 ± 1,683 RLU and 447 ± 14 RLU; MLVpp infectivity values for HepG2-CD81 and HepG2 cells were 193,003 ± 1,873 RLU and 115,300 ± 1,140 RLU. (D) HepG2-CD81 cells were allowed to polarize over 3 days and were treated with serum-free DMEM for 4 h, followed by exposure to control (1:1,000) or Rp-8-Br-cAMPs (50, 100, or 500 mM) for 1 h. Cells were fixed, and the polarity index was enumerated from five fields of view from three independent coverslips.

tissue (Fig. 4), providing support for the use of HepG2 cells as a model system to study HCV entry into polarized hepatocytes.

TJs are dynamically regulated (49), and the major pool(s) of OCLN and ZO-1 in the T84 epithelial cell line is reported to reside in Triton X-100-insoluble raft-like membrane microdomains (39). Similarly, in polarized HepG2 cells we found that the basal and lateral pools of CLDN1 and JAM-A are Triton X-100 soluble, whereas TJ-associated CLDN1 and JAM-A are insoluble to detergent extraction (data not shown). The presence of TJ and nonjunctional pools of CLDNs in the liver is consistent with earlier reports (44). We hypothesize that nonjunctional CLDN1 may be more accessible to interact with the viral glycoproteins during entry. Earlier studies showing that CLDN1 expression in nonpolarized human embryonal 293T kidney cells allow HCVpp entry support a model where entry is not dependent on the formation of functionally active TJs (15, 24, 31, 55, 57). Indeed, the observation that CLDN1 lacking the C-terminal region that is required for transport to the TJs (46) confers viral entry into 293T cells (15, 24) lends further support to a model where nonjunctional CLDN1 has a role in HCV entry.

The expression levels of tagged CLDN1 and CD81 at the basal and lateral membranes of polarized cells were comparable to that of the plasma membrane of nonpolarized HepG2 (Fig. 5B). We (24) and others (11, 55) reported that CLDN1 and CD81 associate at the plasma membrane, suggesting that these complexes play a role in HCV entry. We demonstrate that FRET occurred between membrane-expressed pools of CLDN1 and CD81 at comparable efficiencies in polarized and nonpolarized HepG2 cells to those previously reported in Huh-7 and 293T cells (24), suggesting that receptor complex formation does not limit HCV infection of polarized cells. Interestingly, there was no detectable FRET between TJ-associated pools of CLDN1 and CD81, suggesting that the confor-

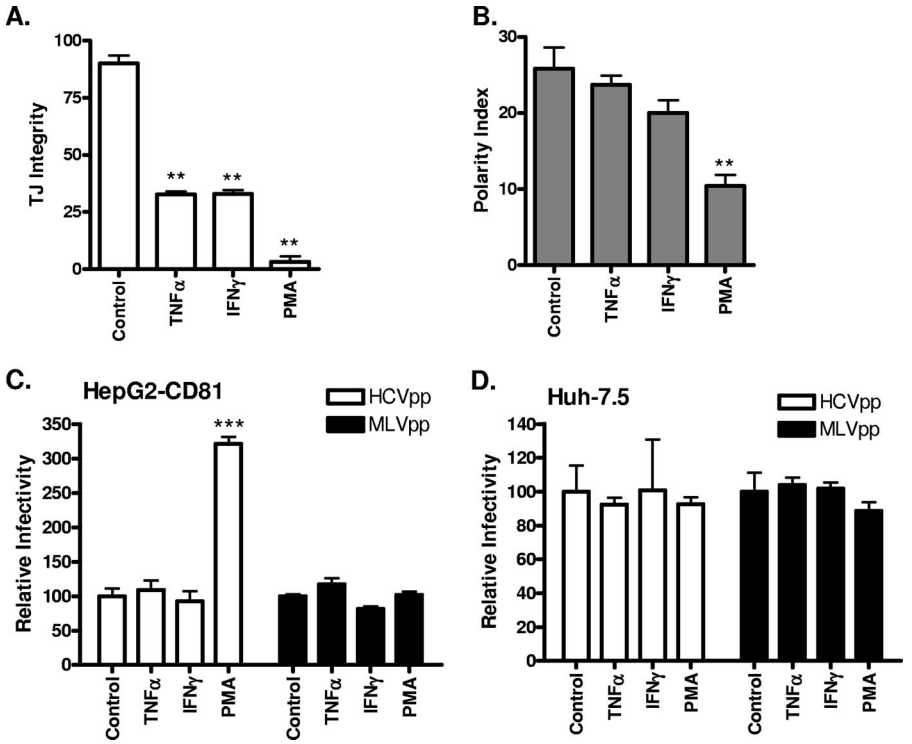

FIG. 7. Effect(s) of proinflammatory cytokines on HepG2 TJ integrity, polarity, and HCV entry. HepG2-CD81 cells were treated with the control (DMSO; 1:1,000), TNF-α (10 ng/ml), IFN-γ (10 ng/ml), or PMA (50 ng/ml) for 24 h. (A) Cells were incubated with CMFDA at 37°C for 10 min and washed, and the capacity of BC lumens to retain CMFDA was monitored by using fluorescence microscopy. TJ integrity was assessed as the percentage of total BC retaining CMFDA (triplicate coverslips, five fields of view per coverslip). **, $P < 0.001$ (*t* test). (B) Cells were fixed, and the number of MRP2-positive BC per 100 cell nuclei was counted (polarity index). HCVpp (white bars) and MLVpp (black bars) infection of control-, TNF-α-, IFN-γ-, or PMA-treated HepG2-CD81 (C) or Huh-7.5 (D) cells is shown relative to control cells ± SD. ***, $P < 0.001$ (*t* test). HCVpp infectivity values for HepG2-CD81, HepG2, and Huh-7.5 cells were 48,350 ± 1,240 RLU, 313 ± 29 RLU, and 149,194 ± 9,869 RLU, respectively. MLVpp infectivity values for HepG2-CD81, HepG2, and Huh-7.5 cells were 349,990 ± 7,075 RLU, 358,400 ± 18,162 RLU, and 727,454 ± 11,673 RLU, respectively.

mation, density, or stoichiometry of the proteins at the TJ is not compatible with coreceptor association. These data are consistent with an earlier report by Kovalenko and colleagues, who demonstrated an association between CLDN1 and the tetraspanin proteins CD81 and CD9 in nonpolarized A431 and A549 epithelial cells (29), leading them to suggest that tetraspanin-enriched microdomains regulate the trafficking of nonjunctional CLDNs (reviewed in reference 21).

We recently demonstrated PKA-dependent localization of CLDN1 in Huh-7 cells, such that inhibiting PKAII reduced CLDN1 membrane expression and abrogated HCV entry (16). To ascertain whether PKA regulates CLDN1 localization at basal and lateral membranes and at TJ domains, HepG2 cells expressing AcGFP.CLDN1 and DsRED.CD81 were treated with the PKA antagonist, Rp-8-Br-cAMPs. Treatment reduced CLDN1 expression at the basal membrane and increased lateral- and TJ-associated forms with no detectable effect on CD81 localization (Fig. 6B). The reduced CLDN1 expression at the basal membrane abrogated FRET association with CD81 at this site. Importantly, Rp-8-Br-cAMPs treatment induced a significant reduction in HCVpp entry. One consequence of HepG2 polarization in vitro, in particular the development of multicellular structures with cells sharing a BC, is the reduced availability of the basal membrane. Quantification of the relative amount of basal and lateral membranes and TJ domains in polarized HepG2 cells demonstrates that as more cells share a BC, the TJ and basal surfaces reduce and the area of lateral membrane increases, supporting the model that basal membrane-expressed pools of receptors have a role in viral entry.

Cytokine-mediated changes in cell permeability contribute to a wide range of pathological conditions, including inflammatory bowel disease, cystic fibrosis, and perturbation of the blood-brain barrier (reviewed in reference 8). While the molecular mechanisms regulating these processes are incompletely understood, model cell culture systems of epithelial/endothelial barrier function have highlighted the important role of cytokines in regulating TJs. Treatment of HepG2-CD81 cells with TNF-α and IFN-γ reduced TJ integrity and yet had a minimal effect on cell polarization or HCVpp entry (Fig. 7). TNF-α and IFN-γ have been reported to modulate actin-myosin contractility and to promote the endocytosis of TJ proteins (reviewed in reference 8). However, the majority of reports have utilized epithelial and endothelial cells with simple polarity, and the effect of cytokines on hepatic permeability is poorly understood. Phorbol ester activation of PKC abrogated TJ integrity and significantly reduced HepG2 polarity, with a concomitant increase in HCVpp infection (Fig. 7). PMA induced a relocalization of CLDN1, ZO-1, and OCLN from TJs, which was not apparent with either cytokine treatment

(data not shown). Several reports demonstrate that PMA activation of PKC can signal a redistribution of TJ proteins from the cell borders to the cytoplasm (9, 18, 38). The signaling events downstream of PKC that regulate cell permeability are incompletely defined; however, multiple components of the TJ complex may be directly phosphorylated by PKC (reviewed in reference 23). These data suggest that functionally intact TJs per se do not limit HCV entry and highlight the differential effect(s) of cytokine and PMA modulation of TJ integrity and protein localization on HCV entry that is worthy of further investigation.

The establishment and maintenance of a fully polarized state requires the appropriate extracellular matrix, cell-cell contacts, and correct geometrical orientation, with many epithelial cells adopting a partially polarized morphology in monolayer culture. Huh-7 hepatoma and clonal derivatives such as Huh-7.5 (5) support high-level HCV RNA replication and are used widely to study HCV infection and entry. We noted heterogeneous expression and localization of CLDN1, OCLN, and JAM-A in Huh-7-derived hepatomas, with frequent breaks in their lateral staining pattern(s). Furthermore, actin staining was heterogeneous, with limited evidence for circumferential bands colocalizing with ZO-1 and JAM-A (unpublished data), as would be expected in a polarized monolayer (33, 35). All treatments to regulate HepG2 polarity had minimal effects on HCVpp or HCVcc infection of Huh-7 or Huh-7.5 cells, in contrast to an earlier report demonstrating that TNF-α induced a redistribution of CLDN1 from the plasma membrane to intracellular sites in Huh-7.5.1 cells (55). Huh-7 cells are heterogeneous with respect to morphology, CD81 expression, and viral RNA replication, and this can change with in vitro passage and culture conditions (1, 28, 32), making data comparison between laboratories difficult. Cumulatively, our data suggest that Huh-7 cells fail to develop mature TJs, explaining the relatively low transepithelial resistance values reported (4, 31) compared to those of more differentiated epithelial cell lines. Recent reports of CLDN1 and OCLN colocalization with ZO-1 at the apex of Huh-7 cells (7, 31) provide insufficient evidence to demonstrate functional TJs, since both ZO-1 and OCLN have been shown to be expressed in cells that lack TJs (14, 47, 54). In contrast, HepG2 cells that develop and maintain complex polarity have been used extensively to define TJ formation and regulation in the development of hepatic polarity (reviewed in references 13 and 53). On the assumption that HepG2 cells mimic hepatocyte polarity within the liver, our data suggest that HCV entry may be suboptimal and that agents which disrupt hepatocyte polarity may promote HCV infection and transmission in the liver.

ACKNOWLEDGMENTS

We thank Charles Rice for J6/JFH, Huh-7.5 cells, and anti-NS5A 9E10, Tianyi Wang for Huh-7 cells, and Stephen Shaw for anti-SRBI.

This work was supported by PHS grants AI50798 and AI40034-14, the MRC, and the Wellcome Trust.

REFERENCES

1. **Akazawa, D., T. Date, K. Morikawa, A. Murayama, M. Miyamoto, M. Kaga, H. Barth, T. F. Baumert, J. Dubuisson, and T. Wakita.** 2007. CD81 expression is important for the permissiveness of Huh7 cell clones for heterogeneous hepatitis C virus infection. J. Virol. **81:**5036–5045.
2. **Barth, H., E. K. Schnober, C. Neumann-Haefelin, C. Thumann, M. B. Zeisel, H. M. Diepolder, Z. Hu, T. J. Liang, H. E. Blum, R. Thimme, M. Lambotin, and T. F. Baumert.** 2008. Scavenger receptor class B is required for hepatitis C virus uptake and cross-presentation by human dendritic cells. J. Virol. **82:**3466–3479.
3. **Bartosch, B., A. Vitelli, C. Granier, C. Goujon, J. Dubuisson, S. Pascale, E. Scarselli, R. Cortese, A. Nicosia, and F. L. Cosset.** 2003. Cell entry of hepatitis C virus requires a set of co-receptors that include the CD81 tetraspanin and the SR-B1 scavenger receptor. J. Biol. Chem. **278:**41624–41630.
4. **Benedicto, I., F. Molina-Jimenez, O. Barreiro, A. Maldonado-Rodriguez, J. Prieto, R. Moreno-Otero, R. Aldabe, M. Lopez-Cabrera, and P. L. Majano.** 2008. Hepatitis C virus envelope components alter localization of hepatocyte tight junction-associated proteins and promote occludin retention in the endoplasmic reticulum. Hepatology **48:**1044–1053.
5. **Blight, K. J., J. A. McKeating, and C. M. Rice.** 2002. Highly permissive cell lines for subgenomic and genomic hepatitis C virus RNA replication. J. Virol. **76:**13001–13014.
6. **Braiterman, L. T., S. Heffernan, L. Nyasae, D. Johns, A. P. See, R. Yutzy, A. McNickle, M. Herman, A. Sharma, U. P. Naik, and A. L. Hubbard.** 2008. JAM-A is both essential and inhibitory to development of hepatic polarity in WIF-B cells. Am. J. Physiol. Gastrointest. Liver Physiol. **294:**G576–G588.
7. **Brazzoli, M., A. Bianchi, S. Filippini, A. Weiner, Q. Zhu, M. Pizza, and S. Crotta.** 2008. CD81 is a central regulator of cellular events required for hepatitis C virus infection of human hepatocytes. J. Virol. **82:**8316–8329.
8. **Capaldo, C. T., and A. Nusrat.** 2009. Cytokine regulation of tight junctions. Biochim. Biophys. Acta **1788:**864–871.
9. **Clarke, H., A. P. Soler, and J. M. Mullin.** 2000. Protein kinase C activation leads to dephosphorylation of occludin and tight junction permeability increase in LLC-PK1 epithelial cell sheets. J. Cell Sci. **113:**3187–3196.
10. **Cormier, E. G., F. Tsamis, F. Kajumo, R. J. Durso, J. P. Gardner, and T. Dragic.** 2004. CD81 is an entry coreceptor for hepatitis C virus. Proc. Natl. Acad. Sci. USA **101:**7270–7274.
11. **Cukierman, L., L. Meertens, C. Bertaux, F. Kajumo, and T. Dragic.** 2009. Residues in a highly conserved claudin-1 motif are required for hepatitis C virus entry and mediate the formation of cell-cell contacts. J. Virol. **83:**5477–5484.
12. **Date, T., T. Kato, M. Miyamoto, Z. Zhao, K. Yasui, M. Mizokami, and T. Wakita.** 2004. Genotype 2a hepatitis C virus subgenomic replicon can replicate in HepG2 and IMY-N9 cells. J. Biol. Chem. **279:**22371–22376.
13. **Decaens, C., M. Durand, B. Grosse, and D. Cassio.** 2008. Which in vitro models could be best used to study hepatocyte polarity? Biol. Cell **100:**387–398.
14. **Dermietzel, R., and D. Krause.** 1991. Molecular anatomy of the blood-brain barrier as defined by immunocytochemistry. Int. Rev. Cytol. **127:**57–109.
15. **Evans, M. J., T. von Hahn, D. M. Tscherne, A. J. Syder, M. Panis, B. Wolk, T. Hatziioannou, J. A. McKeating, P. D. Bieniasz, and C. M. Rice.** 2007. Claudin-1 is a hepatitis C virus co-receptor required for a late step in entry. Nature **446:**801–805.
16. **Farquhar, M. J., H. J. Harris, M. Diskar, S. Jones, C. J. Mee, S. U. Nielsen, C. L. Brimacombe, S. Molina, G. L. Toms, P. Maurel, J. Howl, F. W. Herberg, S. C. van IJzendoorn, P. Balfe, and J. A. McKeating.** 2008. Protein kinase A-dependent step(s) in hepatitis C virus entry and infectivity. J. Virol. **82:**8797–8811.
17. **Farquhar, M. J., and J. A. McKeating.** 2008. Primary hepatocytes as targets for hepatitis C virus replication. J. Viral Hepat. **15:**849–854.
18. **Farshori, P., and B. Kachar.** 1999. Redistribution and phosphorylation of occludin during opening and resealing of tight junctions in cultured epithelial cells. J. Membr. Biol. **170:**147–156.
19. **Feracci, H., T. P. Connolly, R. N. Margolis, and A. L. Hubbard.** 1987. The establishment of hepatocyte cell surface polarity during fetal liver development. Dev. Biol. **123:**73–84.
20. **Flint, M., T. von Hahn, J. Zhang, M. Farquhar, C. T. Jones, P. Balfe, C. M. Rice, and J. A. McKeating.** 2006. Diverse CD81 proteins support hepatitis C virus infection. J. Virol. **80:**11331–11342.
21. **Giepmans, B. N., and S. C. van IJzendoorn.** 2009. Epithelial cell-cell junctions and plasma membrane domains. Biochim. Biophys. Acta **1788:**820–831.
22. **Grove, J., T. Huby, Z. Stamataki, T. Vanwolleghem, P. Meuleman, M. Farquhar, A. Schwarz, M. Moreau, J. S. Owen, G. Leroux-Roels, P. Balfe, and J. A. McKeating.** 2007. Scavenger receptor BI and BII expression levels modulate hepatitis C virus infectivity. J. Virol. **81:**3162–3169.
23. **Harhaj, N. S., and D. A. Antonetti.** 2004. Regulation of tight junctions and loss of barrier function in pathophysiology. Int. J. Biochem. Cell Biol. **36:**1206–1237.
24. **Harris, H. J., M. J. Farquhar, C. J. Mee, C. Davis, G. M. Reynolds, A. Jennings, K. Hu, F. Yuan, H. Deng, S. G. Hubscher, J. H. Han, P. Balfe, and J. A. McKeating.** 2008. CD81 and claudin 1 coreceptor association: role in hepatitis C virus entry. J. Virol. **82:**5007–5020.
25. **Herrema, H., D. Czajkowska, D. Theard, J. M. van der Wouden, D. Kalicharan, B. Zolghadr, D. Hoekstra, and S. C. D. van IJzendoorn.** 2006. Rho kinase, myosin-II, and p42/44 MAPK control extracellular matrix-mediated apical bile canalicular lumen morphogenesis in HepG2 cells. Mol. Biol. Cell **17:**3291–3303.
26. **Hsu, M., J. Zhang, M. Flint, C. Logvinoff, C. Cheng-Mayer, C. M. Rice, and J. A. McKeating.** 2003. Hepatitis C virus glycoproteins mediate pH-depen-

dent cell entry of pseudotyped retroviral particles. Proc. Natl. Acad. Sci. USA **100:**7271–7276.
27. **Konopka, G., J. Tekiela, M. Iverson, C. Wells, and S. A. Duncan.** 2007. Junctional adhesion molecule-A is critical for the formation of pseudocanaliculi and modulates E-cadherin expression in hepatic cells. J. Biol. Chem. **282:**28137–28148.
28. **Koutsoudakis, G., E. Herrmann, S. Kallis, R. Bartenschlager, and T. Pietschmann.** 2007. The level of CD81 cell surface expression is a key determinant for productive entry of hepatitis C virus into host cells. J. Virol. **81:**588–598.
29. **Kovalenko, O. V., X. H. Yang, and M. E. Hemler.** 2007. A novel cysteine cross-linking method reveals a direct association between claudin-1 and tetraspanin CD9. Mol. Cell Proteomics **6:**1855–1867.
30. **Lindenbach, B. D., M. J. Evans, A. J. Syder, B. Wolk, T. L. Tellinghuisen, C. C. Liu, T. Maruyama, R. O. Hynes, D. R. Burton, J. A. McKeating, and C. M. Rice.** 2005. Complete replication of hepatitis C virus in cell culture. Science **309:**623–626.
31. **Liu, S., W. Yang, L. Shen, J. R. Turner, C. B. Coyne, and T. Wang.** 2009. Tight junction proteins claudin-1 and occludin control hepatitis C virus entry and are downregulated during infection to prevent superinfection. J. Virol. **83:**2011–2014.
32. **Lohmann, V., S. Hoffmann, U. Herian, F. Penin, and R. Bartenschlager.** 2003. Viral and cellular determinants of hepatitis C virus RNA replication in cell culture. J. Virol. **77:**3007–3019.
33. **Luo, Y., Y. Zhuo, M. Fukuhara, and L. J. Rizzolo.** 2006. Effects of culture conditions on heterogeneity and the apical junctional complex of the ARPE-19 cell line. Investig. Ophthalmol. Vis. Sci. **47:**3644–3655.
34. **Luzzatto, A. C.** 1981. Hepatocyte differentiation during early fetal development in the rat. Cell Tissue Res. **215:**133–142.
35. **Mandell, K. J., L. Berglin, E. A. Severson, H. F. Edelhauser, and C. A. Parkos.** 2007. Expression of JAM-A in the human corneal endothelium and retinal pigment epithelium: localization and evidence for role in barrier function. Investig. Ophthalmol. Vis. Sci. **48:**3928–3936.
36. **Mee, C. J., J. Grove, H. J. Harris, K. Hu, P. Balfe, and J. A. McKeating.** 2008. Effect of cell polarization on hepatitis C virus entry. J. Virol. **82:**461–470.
37. **Meertens, L., C. Bertaux, L. Cukierman, E. Cormier, D. Lavillette, F. L. Cosset, and T. Dragic.** 2008. The tight junction proteins claudin-1, -6, and -9 are entry cofactors for hepatitis C virus. J. Virol. **82:**3555–3560.
38. **Mullin, J. M., and M. T. McGinn.** 1988. Effects of diacylglycerols on LLC-PK1 renal epithelia: similarity to phorbol ester tumor promoters. J. Cell Physiol. **134:**357–366.
39. **Nusrat, A., C. A. Parkos, P. Verkade, C. S. Foley, T. W. Liang, W. Innis-Whitehouse, K. K. Eastburn, and J. L. Madara.** 2000. Tight junctions are membrane microdomains. J. Cell Sci. **113:**1771–1781.
40. **Paris, L., L. Tonutti, C. Vannini, and G. Bazzoni.** 2008. Structural organization of the tight junctions. Biochim. Biophys. Acta **1778:**646–659.
41. **Pichard, L., E. Raulet, G. Fabre, J. B. Ferrini, J. C. Ourlin, and P. Maurel.** 2006. Human hepatocyte culture. Methods Mol. Biol. **320:**283–293.
42. **Piontek, J., L. Winkler, H. Wolburg, S. L. Muller, N. Zuleger, C. Piehl, B. Wiesner, G. Krause, and I. E. Blasig.** 2008. Formation of tight junction: determinants of homophilic interaction between classic claudins. FASEB J. **22:**146–158.
43. **Ploss, A., M. J. Evans, V. A. Gaysinskaya, M. Panis, H. You, Y. P. de Jong, and C. M. Rice.** 2009. Human occludin is a hepatitis C virus entry factor required for infection of mouse cells. Nature **457:**882–886.
44. **Rahner, C., M. Fukuhara, S. Peng, S. Kojima, and L. J. Rizzolo.** 2004. The apical and basal environments of the retinal pigment epithelium regulate the maturation of tight junctions during development. J. Cell Sci. **117:**3307–3318.
45. **Reynolds, G. M., L. J. Billingham, L. J. Gray, J. R. Flavell, S. Najafipour, J. Crocker, P. Nelson, L. S. Young, and P. G. Murray.** 2002. Interleukin 6 expression by Hodgkin/Reed-Sternberg cells is associated with the presence of 'B' symptoms and failure to achieve complete remission in patients with advanced Hodgkin's disease. Br. J. Haematol. **118:**195–201.
46. **Rüffer, C., A. Strey, A. Janning, K. S. Kim, and V. Gerke.** 2004. Cell-cell junctions of dermal microvascular endothelial cells contain tight and adherens junction proteins in spatial proximity. Biochemistry **43:**5360–5369.
47. **Saitou, M., K. Fujimoto, Y. Doi, M. Itoh, T. Fujimoto, M. Furuse, H. Takano, T. Noda, and S. Tsukita.** 1998. Occludin-deficient embryonic stem cells can differentiate into polarized epithelial cells bearing tight junctions. J. Cell Biol. **141:**397–408.
48. **Scarselli, E., H. Ansuini, R. Cerino, R. M. Roccasecca, S. Acali, G. Filocamo, C. Traboni, A. Nicosia, R. Cortese, and A. Vitelli.** 2002. The human scavenger receptor class B type I is a novel candidate receptor for the hepatitis C virus. EMBO J. **21:**5017–5025.
49. **Shen, L., C. R. Weber, and J. R. Turner.** 2008. The tight junction protein complex undergoes rapid and continuous molecular remodeling at steady state. J. Cell Biol. **181:**683–695.
50. **Stamataki, Z., J. Grove, P. Balfe, and J. A. McKeating.** 2008. Hepatitis C virus entry and neutralization. Clin. Liver Dis. **12:**693–712.
51. **Théard, D., M. Steiner, D. Kalicharan, D. Hoekstra, and S. C. van IJzendoorn.** 2007. Cell polarity development and protein trafficking in hepatocytes lacking E-cadherin/β-catenin-based adherens junctions. Mol. Biol. Cell **18:**2313–2321.
52. **Wakita, T., T. Pietschmann, T. Kato, T. Date, M. Miyamoto, Z. Zhao, K. Murthy, A. Habermann, H. G. Krausslich, M. Mizokami, R. Bartenschlager, and T. J. Liang.** 2005. Production of infectious hepatitis C virus in tissue culture from a cloned viral genome. Nat. Med. **11:**791–796.
53. **Wang, L., and J. L. Boyer.** 2004. The maintenance and generation of membrane polarity in hepatocytes. Hepatology **39:**892–899.
54. **Williams, C. D., and L. J. Rizzolo.** 1997. Remodeling of junctional complexes during the development of the outer blood-retinal barrier. Anat. Rec. **249:**380–388.
55. **Yang, W., C. Qiu, N. Biswas, J. Jin, S. C. Watkins, R. C. Montelaro, C. B. Coyne, and T. Wang.** 2008. Correlation of the tight junction-like distribution of Claudin-1 to the cellular tropism of hepatitis C virus. J. Biol. Chem. **283:**8643–8653.
56. **Zegers, M. M., and D. Hoekstra.** 1998. Mechanisms and functional features of polarized membrane traffic in epithelial and hepatic cells. Biochem. J. **336:**257–269.
57. **Zheng, A., F. Yuan, Y. Li, F. Zhu, P. Hou, J. Li, X. Song, M. Ding, and H. Deng.** 2007. Claudin-6 and claudin-9 function as additional coreceptors for hepatitis C virus. J. Virol. **81:**12465–12471.
58. **Zhong, J., P. Gastaminza, G. Cheng, S. Kapadia, T. Kato, D. R. Burton, S. F. Wieland, S. L. Uprichard, T. Wakita, and F. V. Chisari.** 2005. Robust hepatitis C virus infection in vitro. Proc. Natl. Acad. Sci. USA **102:**9294–9299.